The type III effector HopF2$_{Pto}$ targets *Arabidopsis* RIN4 protein to promote *Pseudomonas syringae* virulence

Mike Wilton[a], Rajagopal Subramaniam[b], James Elmore[c], Corinna Felsensteiner[a,d], Gitta Coaker[c], and Darrell Desveaux[a,d,1]

[a]Department of Cell and Systems Biology and [d]Centre for the Analysis of Genome Evolution and Function, University of Toronto, Toronto, ON M5S 3B2, Canada; [b]Agriculture and Agri-Food Canada/Agriculture et Agroalimentaire Canada, Ottawa, ON K1A 0C6, Canada; and [c]Department of Plant Pathology, University of California, Davis, CA 95616

Edited by Jeffery L. Dangl, University of North Carolina, Chapel Hill, NC, and approved December 9, 2009 (received for review April 29, 2009)

Plant immunity can be induced by two major classes of pathogen-associated molecules. Pathogen- or microbe-associated molecular patterns (PAMPs or MAMPs) are conserved molecular components of microbes that serve as "non-self" features to induce PAMP-triggered immunity (PTI). Pathogen effector proteins used to promote virulence can also be recognized as "non-self" features or induce a "modified-self" state that can induce effector-triggered immunity (ETI). The *Arabidopsis* protein RIN4 plays an important role in both branches of plant immunity. Three unrelated type III secretion effector (TTSE) proteins from the phytopathogen *Pseudomonas syringae*, AvrRpm1, AvrRpt2, and AvrB, target RIN4, resulting in ETI that effectively restricts pathogen growth. However, no pathogenic advantage has been demonstrated for RIN4 manipulation by these TTSEs. Here, we show that the TTSE HopF2$_{Pto}$ also targets *Arabidopsis* RIN4. Transgenic plants conditionally expressing HopF2$_{Pto}$ were compromised for AvrRpt2-induced RIN4 modification and associated ETI. HopF2$_{Pto}$ interfered with AvrRpt2-induced RIN4 modification in vitro but not with AvrRpt2 activation, suggestive of RIN4 targeting by HopF2$_{Pto}$. In support of this hypothesis, HopF2$_{Pto}$ interacted with RIN4 in vitro and in vivo. Unlike AvrRpm1, AvrRpt2, and AvrB, HopF2$_{Pto}$ did not induce ETI and instead promoted *P. syringae* growth in *Arabidopsis*. This virulence activity was not observed in plants genetically lacking RIN4. These data provide evidence that RIN4 is a major virulence target of HopF2$_{Pto}$ and that a pathogenic advantage can be conveyed by TTSEs that target RIN4.

bacterial virulence | type III secretion

An important virulence strategy adopted by bacterial phytopathogens is the suppression of plant immunity (1, 2). To accomplish this, Gram-negative bacterial phytopathogens such as *Pseudomonas syringae* translocate type III secretion effector (TTSE) proteins into the host cytosol via the type III secretion system (TTSS) (3). Several of these TTSEs have demonstrated the ability to suppress plant immunity by targeting important defense-related proteins thereby promoting pathogen growth (reviewed in ref. 1). In response, it is likely that the selective pressures imposed by pathogen effector proteins have contributed to shaping and driving the evolution of effective plant immune responses (4).

Plant effector-triggered immunity (ETI) occurs when specific pathogen effector proteins are detected by plant resistance (R) proteins, which activate an effective resistance response that often culminates in a localized programmed cell death termed the hypersensitive response (HR) (5, 6). The recognition of effectors by R proteins can occur by either direct or indirect interactions (7). In a number of cases described so far, R proteins recognize modifications of host proteins induced by the activity of effector proteins and subsequently induce ETI (6, 8).

The *Arabidopsis* RPM1-interacting protein (RIN4) is a negative regulator of PAMP-triggered immunity (PTI) that interacts with two R proteins, RPM1 and RPS2 (9–12). Three unrelated *P. syringae* type III effectors, AvrRpm1, AvrRpt2, and AvrB, have been demonstrated to target RIN4 (10–12). The R protein RPM1 can recognize the presence of both AvrB and AvRpm1, whereas RPS2 recognizes AvrRpt2. RIN4 is phosphorylated in response to infection by either AvrB or AvrRpm1, leading to the activation of RPM1 (10). However, kinase activity has not been demonstrated for either AvrB or AvrRpm1 and therefore the phosphorylation may be indirect (13–15). AvrRpt2 belongs to the CA-clan of cysteine proteases (16). Upon translocation into the plant cell, host cyclophilins, like *Arabidopsis* ROC1, activate AvrRpt2 protease activity (17, 18). Activated AvrRpt2 undergoes autoprocessing of 71 amino acids from its N terminus to yield the mature protease (17, 19). AvrRpt2 then cleaves RIN4 at two sequences similar to its autoprocessing site (20–22). Cleavage of RIN4 is believed to activate RPS2 leading to ETI (11, 12). Both recognition events by RPM1 and RPS2 are to the bacteria's detriment, which raises the question of why these pathogenic TTSEs target RIN4. In fact, AvrRpm1, AvrRpt2, and AvrB all retain virulence functions in the absence of RIN4 and their corresponding resistance proteins (23). Therefore, it remains to be determined whether TTSE manipulation of RIN4 can promote pathogen virulence or whether RIN4 is a decoy for the true virulence targets of TTSEs (24).

The *HopF2* (formerly HopPtoF) locus of *P. syringae* pv. *tomato* DC3000 (*Pto* DC3000) encodes two genes, the type III chaperone *schF*$_{Pto}$ and the type III effector *hopF2*$_{Pto}$ (25). H*opF2*$_{Pto\ DC3000}$ (hereafter referred to as *HopF2*$_{Pto}$) uses a rare ATA translation initiation codon that limits protein production in *P. syringae* (25). Mutation of the native ATA start codon to ATG results in HopF2$_{Pto}$-mediated virulence in tomato (26). HopF2$_{Pto}$ possesses a predicted myristoylation sequence that is required for localization to the plasma membrane of onion epidermal cells (26). Moreover, HopF2$_{Pto}$ avirulence in tobacco W38 and virulence in tomato require an intact myristoylation sequence, suggesting that HopF2$_{Pto}$ functions at the plasma membrane (26). HopF2$_{Pto}$ can suppress PTI in *Nicotiana benthamiana,* flagellin-induced *NON-HOST1* (*NHO1*) induction in *Arabidopsis* protoplasts, callose deposition in transgenic *Arabidopsis* expressing HopF2$_{Pto}$, and also the HopA1 (formerly HopPsyA)-induced HR in the *A. thaliana* ecotype Ws-0 (27–30). However, the biochemical function and host target(s) of HopF2$_{Pto}$ remain to be elucidated.

HopF1$_{Pph7}$ from *P. syringae* pv. *phaseolicola* race 7 (1449B) shares 48% amino acid identity with HopF2$_{Pto}$ and displays virulence or avirulence functions on various bean cultivars (31–33).

Author contributions: M.W., R.S., J.E., G.C., and D.D. designed research; M.W., R.S., J.E., C.F., G.C., and D.D. performed research; M.W., R.S., J.E., G.C., and D.D. analyzed data; and M.W. and D.D. wrote the paper.

The authors declare no conflict of interest.

This article is a PNAS Direct Submission.

[1]To whom correspondence should be addressed. E-mail: darrell.desveaux@utoronto.ca.

This article contains supporting information online at www.pnas.org/cgi/content/full/0904739107/DCSupplemental.

The crystal structure of HopF1$_{Pph7}$ shares limited structural homology to the catalytic domain of bacterial ADP ribosyltransferases (ADP-RT), yet no ADP-RT activity could be demonstrated in vitro (33). Nevertheless, the structural similarity identified a conserved pocket with two amino acids that share structural similarity to catalytic residues of the ADP ribosyltransferase diphtheria toxin, R72 and D174. Mutational analysis of these residues abolished the avirulence and virulence functions of HopF1$_{Pph7}$ in the bean cultivars Red Mexican and Tendergreen, respectively, demonstrating their importance for HopF function (33).

To gain insights into HopF function and putative host targets, we examined *HopF2$_{Pto}$* transgenic *Arabidopsis* plants for altered immunity. *Arabidopsis* plants expressing HopF2$_{Pto}$ are compromised for AvrRpt2-induced ETI. Furthermore, HopF2$_{Pto}$ can interfere with AvrRpt2-induced RIN4 cleavage in vivo and in vitro, suggesting that HopF2$_{Pto}$ may target RIN4. In support of this hypothesis, HopF2$_{Pto}$ interacts with RIN4 both in vivo and in vitro. We also demonstrate that HopF2$_{Pto}^{ATG}$ can enhance the growth of *P. syringae* in *Arabidopsis*. The virulence function in *Arabidopsis* depends on the conserved amino acids important for both avirulence and virulence functions of HopF1$_{Pph7}$ in bean cultivars. Importantly, RIN4 is required for HopF2$_{Pto}$-enhanced *P. syringae* growth, indicating that RIN4 is a major virulence target of the TTSE HopF2$_{Pto}$.

Results

HopF2$_{Pto}$-Expressing *Arabidopsis* Plants Are Compromised for AvrRpt2-Mediated Effector-Triggered Immunity (ETI). Transgenic *Arabidopsis thaliana* ecotype Col-0 capable of dexamethasone (DEX)-inducible *hopF2$_{Pto}$* or *hopF2$_{Pto}^{D175A}$* (corresponding to HopF1$_{Pph7}$ D174) expression were created with a C-terminal translational fusion to an HA epitope tag (Fig. S1) (34). To assess whether HopF2$_{Pto}$:HA can delay or suppress the HR associated with ETI, *Pto* DC3000 expressing various avirulence genes were infiltrated into HopF2$_{Pto}$:HA transgenic plants. AvrRpt2-mediated HR was suppressed in HopF2$_{Pto}$-expressing plants, whereas the HR induced by AvrB, AvrRpm1, or HopZ1a$_{PsyA2}$ was indistinguishable from untreated transgenic plants (Fig. 1*A*). Loss of AvrRpt2-mediated HR was also observed in two additional independent transgenic lines expressing HopF2$_{Pto}$ (Fig. S1). AvrRpt2-mediated HR suppression was not observed in two independent transgenic lines expressing the mutant HopF2$_{Pto}^{D175A}$ (Fig. S1). The suppression of cell death associated with AvrRpt2-mediated HR was confirmed by Trypan blue staining and electrolyte leakage experiments (Fig. 1 *B* and *C*). In addition, loss of AvrRpt2-induced HR was associated with suppression of AvrRpt2-induced ETI as monitored by bacterial growth (Fig. 1*D* and Fig. S8). The loss of AvrRpt2-induced resistance was not observed in DEX-treated HopF2$_{Pto}^{D175A}$:HA transgenic plants (Fig. 1*D*). Therefore, HopF2$_{Pto}$ effectively suppresses AvrRpt2-induced HR and ETI, and this activity depends on the conserved residue D175. Because AvrRpt2 is known to target *Arabidopsis* RIN4 protein, we examined whether HopF2$_{Pto}$ interferes with AvrRpt2-induced RIN4 modifications.

HopF2$_{Pto}$ Inhibits AvrRpt2-Mediated RIN4 Degradation in Vivo and in Vitro. The HR elicited by AvrRpt2 is associated with a rapid depletion of RIN4 within 8 h of inoculation, which is thought to be required for AvrRpt2-mediated ETI (11, 12). To test whether HopF2$_{Pto}$ attenuates AvrRpt2-mediated RIN4 depletion, RIN4 levels were monitored in HopF2$_{Pto}$:HA and HopF2$_{Pto}^{D175A}$:HA transgenic leaves inoculated with *Pto* DC3000 expressing AvrRpt2 (Fig. 2*A*). In uninduced leaves, RIN4 levels decreased significantly by 2 h postinfection, whereas in DEX-treated leaves RIN4 levels persisted without a detectable decrease up to 24 h after bacterial inoculation. In HopF2$_{Pto}^{D175A}$:HA-expressing tissues, RIN4 disappearance was still observed (Fig. 2*A*).

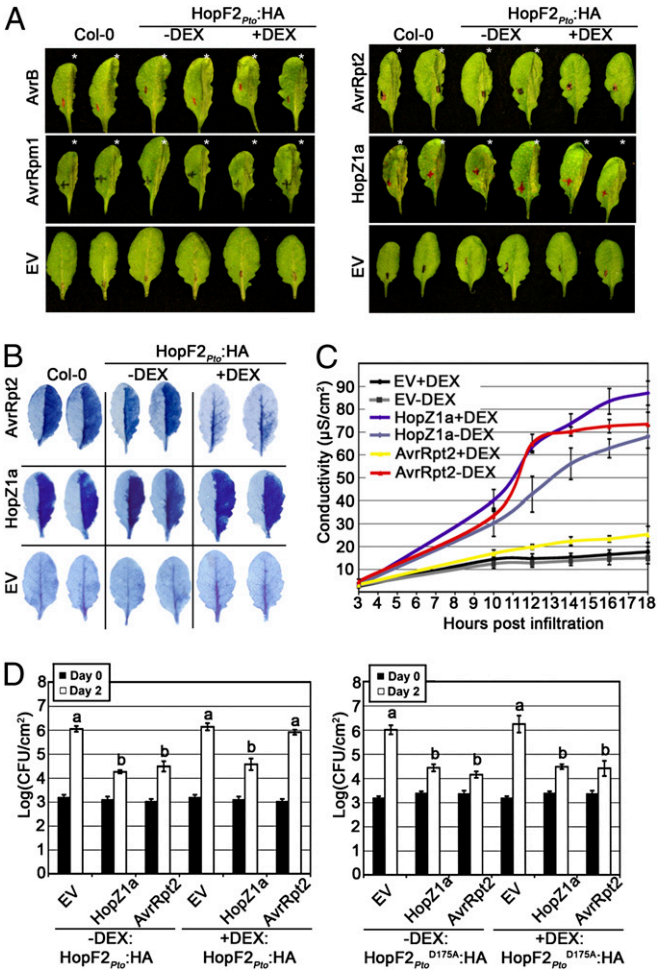

Fig. 1. Transgenic expression of HopF2$_{Pto}$ suppresses AvrRpt2-mediated ETI. (*A*) Half-leaves of untreated HopF2$_{Pto}$ transgenic plants (−DEX) or HopF2$_{Pto}$ transgenic plants treated with DEX for 24 h (+DEX) were infiltrated with *Pto* DC3000 (5×10^7 cfu/mL) expressing the indicated avirulence gene or empty vector (EV). Photographs of AvrB, AvrRpm1, or corresponding EV control were taken 6 h after inoculation, whereas HopZ1a$_{PsyA2}$, AvrRpt2, or corresponding EV were taken ≈20 h after inoculation. Asterisks indicate leaves with visible HR collapse. (*B*) Trypan blue staining of untreated (−DEX) or 24 h DEX-treated (+DEX) HopF2$_{Pto}$ transgenic leaves 14 h postinoculation. (*C*) Electrolyte leakage of untreated (−DEX) or 24 h DEX-treated (+DEX) HopF2$_{Pto}$ transgenic leaf disks after infiltration with *Pto* DC3000 expressing the indicated constructs. (*D*) Growth analysis of *Pto* DC3000 expressing the indicated avirulence gene or the empty vector (EV) infiltrated into HopF2$_{Pto}$ or HopF2$_{Pto}^{D175A}$ transgenic plants. Plants were treated with 30 μM DEX (+DEX) or water (−DEX) immediately after bacterial inoculation. Bacterial counts were performed 1 h postinoculation (day 0; filled bars) and 2 days postinoculation (day 2; open bars). Although *Pto* DC3000 empty vector did not grow significantly better in DEX-treated HopF2$_{Pto}$:HA plants after 2 days of growth, a significant growth enhancement was observed after 3 days of growth (Fig. S7). Results are representative of three independent replicates. Error bars represent the SD from eight samples. "a" or "b" above the bar denotes statistically significant [Fisher's protected least significant difference post hoc (FLSD) test, $P < 0.05$] differences between samples. Similar results were obtained with an independent transgenic HopF2$_{Pto}$ line, as well with a lower DEX concentration of 3 μM (Fig. S8).

Because HopF2$_{Pto}$ interferes with AvrRpt2-mediated cleavage of RIN4 *in planta* (Fig. 2*A*), we performed a series of in vitro cleavage reactions using purified recombinant proteins to analyze the effect of HopF2$_{Pto}$ on AvrRpt2 activation and RIN4 cleavage. As previously shown, incubation of AvrRpt2:HA with GST:ROC1 resulted in activation of AvrRpt2:HA and self-processing as

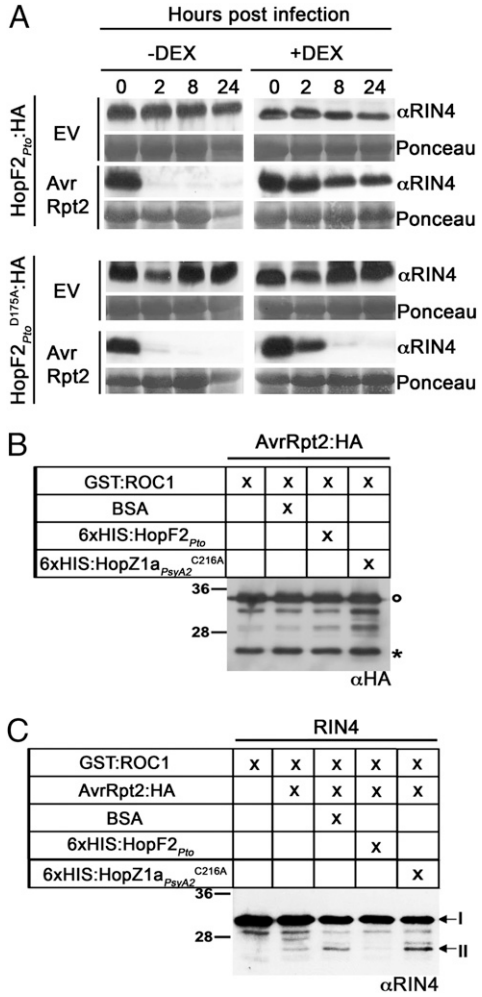

Fig. 2. HopF2$_{Pto}$ inhibits AvrRpt2-mediated degradation of RIN4. (*A*) Immunoblot analysis of RIN4 levels in *Arabidopsis* HopF2$_{Pto}$ and HopF2$_{Pto}^{D175A}$ transgenic leaves infiltrated with *Pto* DC3000 empty vector (EV) or *Pto* DC3000 expressing AvrRpt2. Expression of HopF2$_{Pto}$:HA or HopF2$_{Pto}^{D175A}$:HA was induced with 30 μM DEX 24 h before infection. *Pto* DC3000 was infiltrated at 5×10^7 cfu/mL, and samples were collected at the indicated time after infiltration. (*B*) HopF2$_{Pto}$ does not inhibit AvrRpt2 activation and self-processing in vitro. In vitro cleavage reactions (see *Methods*) were probed with HA antisera. Cleavage reactions were performed five times with similar results. ○, full-length AvrRpt2; *, processed AvrRpt2. (*C*) HopF2$_{Pto}$ interferes with AvrRpt2-mediated RIN4 proteolysis in vitro. Reactions were conducted as in *B* and probed with RIN4 antisera. Arrows indicate full-length RIN4 (I) and proteolytically cleaved RIN4 (II).

indicated by the presence of an ≈21-kDa band corresponding to the C-terminal portion of AvrRpt2:HA (asterisk in Fig. 2*B*) (17). The addition of recombinant 6xHIS:HopF2$_{Pto}$ had no effect on the ability of GST:ROC1 to activate AvrRpt2:HA, indicating that HopF2$_{Pto}$ does not interfere with the activation of AvrRpt2 (Fig. 2*B*). When recombinant 6xHIS:HopF2$_{Pto}$ was incubated with RIN4, GST:ROC1, and AvrRpt2:HA, cleaved RIN4 product was greatly diminished relative to the control reactions (Fig. 2*C*), whereas BSA or the recombinant protein 6xHIS: HopZ1a$_{PsyA2}^{C216A}$ did not interfere with the proteolytic cleavage of RIN4 (II, Fig. 2*C*) (20–22). These results suggest that HopF2$_{Pto}$ hinders the ability of activated AvrRpt2 to cleave RIN4 in vitro.

HopF2$_{Pto}$ Interacts with RIN4 in Vitro and in Vivo. To test whether HopF2$_{Pto}$ directly interacts with RIN4, recombinant GST:RIN4 or GST was incubated with 6xHIS:HopF2$_{Pto}$ and precipitated with glutathione GST-binding resin (Fig. 3*A* and Fig. S9). Equal amounts of purified 6xHIS:HopF2$_{Pto}$ recombinant protein were added to either GST:RIN4- or GST-bound glutathione beads. Only GST:RIN4 provided an enrichment of 6xHIS:HopF2$_{Pto}$ upon precipitation, indicating that recombinant RIN4 interacts with HopF2$_{Pto}$ in vitro (Fig. 3*A*). To determine whether HopF2$_{Pto}$ and RIN4 interact in vivo, DEX-induced and uninduced HopF2$_{Pto}$:HA transgenic leaves were subjected to immunoprecipitation with anti-RIN4 antibodies. HopF2$_{Pto}$:HA was detectable in the induced fraction immunoprecipitated with anti-RIN4 sera (Fig. 3*C*). Conversely, RIN4 was detectable in the induced fraction immunoprecipitated with anti-HA antibodies but not in the uninduced fraction or in fractions immunoprecipitated with uncoupled magnetic beads (Fig. 3 *B* and *C* and Fig. S2*A*). Immunoprecipitations carried out

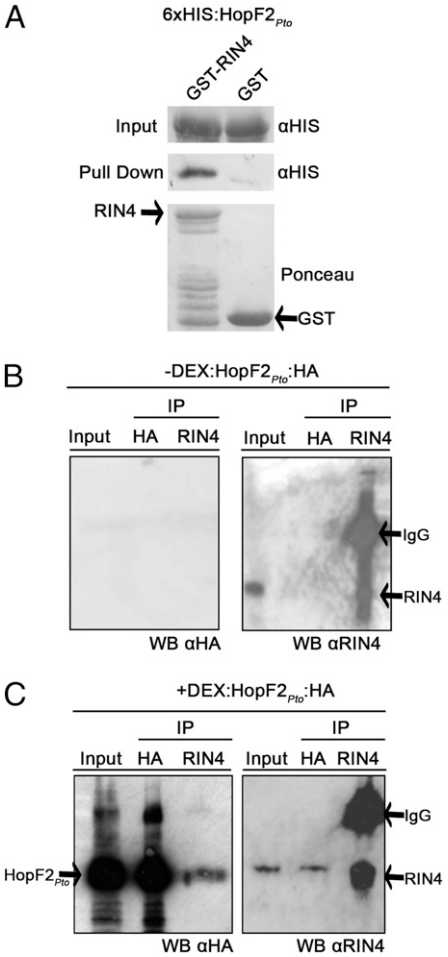

Fig. 3. HopF2$_{Pto}$ interacts with RIN4 both in vitro and in vivo. (*A*) GST:RIN4- or GST-bound glutathione resin was incubated with recombinant 6xHIS:HopF2$_{Pto}$, washed and probed for the presence of bound 6xHIS:HopF2$_{Pto}$ (see *Methods*). Equal volumes of 6xHIS:HopF2$_{Pto}$ added to GST:RIN4- or GST-bound glutathione resin were immunoblotted and probed with HIS antisera before washes (*Top*) or following washes (*Middle*). (*Bottom*) Ponceau stain before washes as a loading control. The GST and full-length RIN4 bands are indicated by an arrow. Bands below the full-length RIN4 band are RIN4 degradation products as determined by an anti-RIN4 blot (Fig. S9). (*B* and *C*) HopF2$_{Pto}$ associates with RIN4 in vivo. (*B*) Uninduced HopF2$_{Pto}$ transgenic leaves were harvested 24 h after mock treatment. Ten micrograms of input protein (Input) or entire elution (50 μL) of the immunoprecipitation (IP) by α-HA or α-RIN4 was loaded onto the SDS/PAGE gel and probed with the indicated antisera (see *Methods*). (*C*) HopF2$_{Pto}$ transgenic leaves were harvested 24 h after 30 μM DEX application and treated as described in *B*. α-HA immunoblot detects the presence of HopF2$_{Pto}$:HA.

using the stringent RIPA wash buffer showed no marked decrease in the amounts of RIN4 immunoprecipitated with HopF2$_{Pto}$:HA, indicating that the interaction between HopF2$_{Pto}$ and RIN4 or a RIN4 complex is specific (Fig. S2*B*) (35). Collectively, these results indicate that HopF2$_{Pto}$ interacts with RIN4 or a RIN4-associated complex in vivo.

HopF2$_{Pto}$ Promotes RIN4-Dependent *P. syringae* Growth in *Arabidopsis*. Previous characterization of HopF2$_{Pto}$ virulence function in tomato revealed that growth advantages to *hopF2*$^{-}$ mutant of *Pto* DC3000 complemented with the *hopF2*$_{Pto}$ gene (*schF2* and *hopF2*) could be enhanced by replacing the native ATA start codon of *HopF2*$_{Pto}$ with an ATG start codon (26). Similarly, expression of *schF2*/*hopF2*^{ATG}*:HA* in the *HopF2*$^{-}$ *Pto* DC3000 strain resulted in a significant growth advantage of 5-fold in *Arabidopsis* ecotype Col-0 compared to the empty vector control or *schF2*/*hopF2*^{ATA}*:HA* (Fig. 4*A* and Fig. S3). The amino acid residues R71 and D175 of HopF2$_{Pto}^{ATG}$ (corresponding to residues R72 and D174 of HopF1$_{Pph7}$) were required for *HopF2*$_{Pto}$ virulence function in *Arabidopsis* (Fig. 4*A*). Mutation of the predicted myristoylation site (HopF2$_{Pto}^{G2A}$) also compromised HopF2$_{Pto}^{ATG}$:HA virulence function (Fig. 4*B*) (26). Loss of virulence function could not be attributed to lack of expression because HopF2$_{Pto}^{ATG/R71A}$:HA, HopF2$_{Pto}^{ATG/D175A}$:HA, and HopF2$_{Pto}^{ATG/G2A}$:HA were expressed to similar levels as wild-type HopF2$_{Pto}^{ATG}$:HA in *P. syringae* (Fig. 4*C*). Therefore, we conclude that HopF2$_{Pto}^{ATG}$:HA-enhanced *P. syringae* growth in *Arabidopsis* requires intact conserved residues R71 and D175, as well as the myristoylation sequence. This suggests that a membrane localized virulence target may be modified by the action of HopF2$_{Pto}$.

To determine whether RIN4 is required for HopF2$_{Pto}$-mediated virulence, we examined the growth of *P. syringae*-expressing HopF2$_{Pto}^{ATG}$:HA in *Arabidopsis* plants that genetically lack RIN4. Because RIN4 is a negative regulator of RPS2, both *RIN4* and *RPS2* must be lacking to prevent the lethality associated with activation of RPS2 (11). We observed that HopF2$_{Pto}^{ATG}$:HA conferred no growth advantage to the *HopF2*$^{-}$ mutant of *Pto* DC3000 in *rin4*/*rps2* or *rpm1*/*rin4*/*rps2* (Fig. 4*D*), indicating that RIN4 is required for HopF2$_{Pto}$ virulence function in *Arabidopsis*. HopF2$_{Pto}^{ATG}$:HA virulence function did not require RPM1 or RPS2 because the growth advantage conferred to *Pto* DC3000 expressing HopF2$_{Pto}^{ATG}$:HA, was retained in *rps2* and *rpm1 Arabidopsis* plants (Fig. 4*E*). Together, these results demonstrate that HopF2$_{Pto}^{ATG}$:HA virulence activity in *Arabidopsis* depends on RIN4 and not the RIN4-associated R proteins RPM1 and RPS2.

Discussion

In this study, we sought to identify potential host targets of the HopF family of phytopathogenic TTSE proteins. Transgenic HopF2$_{Pto}$-expressing *Arabidopsis* plants were compromised for AvrRpt2-induced ETI and HR (Fig. 1). HopF2$_{Pto}$ interfered with AvrRpt2-mediated cleavage of RIN4 *in planta* and in vitro (Fig. 2), and interacted with RIN4 *in planta* and in vitro (Fig. 3). The marked difference between the immunoprecipitation and the coimmunoprecipitation suggests that only a subset of *Arabidopsis* RIN4 is targeted by HopF (Fig. 3 *B* and *C*). The *hopF*$^{-}$ mutant of *Pto* DC3000 did not show decreased virulence in *Arabidopsis* relative to wild-type *Pto* DC3000, possibly because of the functional redundancy of TTSE functions (Fig. S4) (1). However, overexpression of HopF2$_{Pto}^{ATG}$ in this strain by changing the native ATA start codon to ATG conferred a growth advantage in wild-type *Arabidopsis* Col-0 plants but not in *rin4*/*rps2* or *rin4*/*rps2*/*rpm1* plants genetically lacking RIN4 (Fig. 4). Overall, these results support a model where overexpressed HopF2$_{Pto}$ targets *Arabidopsis* RIN4 protein to promote pathogen growth.

Transgenic expression of HopF2$_{Pto}$ effectively suppressed AvrRpt2-mediated HR (Fig. 1), In contrast, *Pto* DC3000 naturally expresses HopF2$_{Pto}$ and has long been used to elicit AvrRpt2-

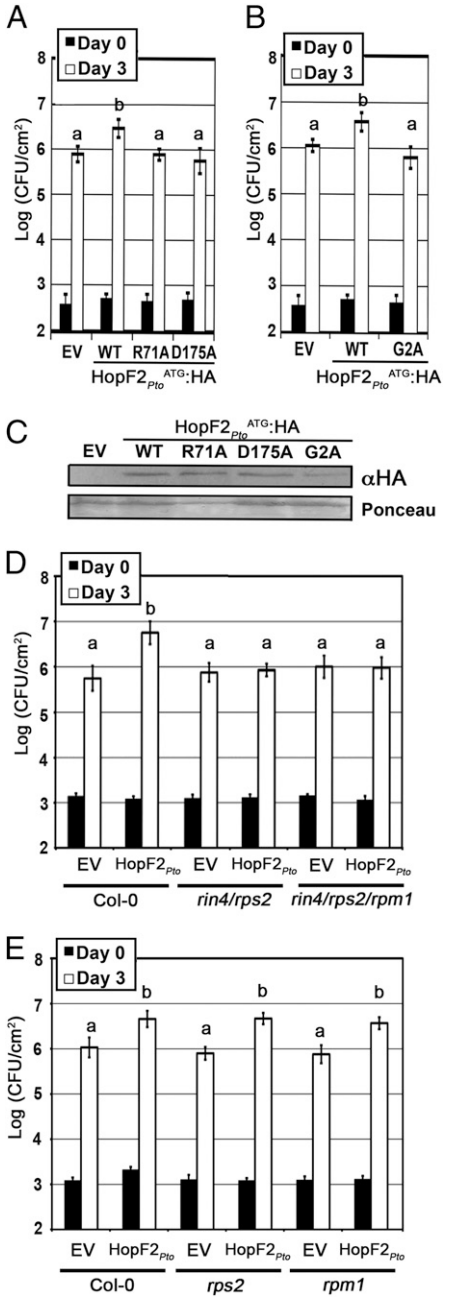

Fig. 4. HopF2$_{Pto}$ virulence function requires the RIN4 *Arabidopsis* protein. (*A* and *B*) Growth of *Pto* DC3000 *hopF2*$^{-}$ mutant expressing the indicated HopF2$_{Pto}^{ATG}$ construct or the empty vector (EV) in *Arabidopsis* Col-0 leaves. Bacterial counts were performed 1 h postinoculation (day 0; filled bars) and 3 days postinoculation (day 3; open bars). Error bars represent the SD of eight samples. Experiments are representative of three independent trials. "a" or "b" above a bar denotes statistically significant [Fisher's protected least significant difference post hoc (FLSD) test, $P < 0.05$] differences between samples. (*C*) Immunoblot analysis of indicated HopF2$_{Pto}^{ATG}$:HA protein expression in the *Pto hopF2*$^{-}$ mutant. Bacteria were grown in minimal media to induce the type III secretion system, and equal amounts of protein were immunoblotted with HA antisera (33). Ponceau red staining is shown as a loading control. (*D* and *E*) Growth of *Pto* DC3000 *hopF2*$^{-}$ mutant expressing HopF2$_{Pto}^{ATG}$:HA (HopF2$_{Pto}$) or the empty vector (EV) in *Arabidopsis* Col-0 wild-type, *rin4*/*rps2*, *rin4*/*rps2*/*rpm1*, *rps2*, or *rpm1* leaves. Bacterial counts were performed as in *A* and *B*. This experiment is representative of three independent trials.

mediated HR in *Arabidopsis*. Furthermore, we also observed that *Pto* DC3000 expressing HopF2$_{Pto}^{ATG}$ could not inhibit AvrRpt2-mediated HR and associated RIN4 degradation in bacterial mixing experiments or when expressed in the *Pto* JL1065, which natively induces an AvrRpt2-mediated HR (Fig. S5) (36, 37). Together, these results indicate an important difference between what HopF2$_{Pto}$ can do when expressed *in planta* transgenically versus what it does when delivered from *P. syringae*. One possible explanation for this difference is that AvrRpt2 HR suppression requires an *in planta* threshold level of HopF2$_{Pto}$ that is attained by transgenic expression but not bacterial delivery (even with the ATG start codon). Another possibility is that bacterially delivered AvrRpt2 and HopF2$_{Pto}^{ATG}$ activities are temporally distinct, similar to the *Salmonella* type III effectors SopE and SptP; however, transgenic expression of HopF2$_{Pto}^{ATG}$ negates this difference (38). In addition, bacterially delivered HopF2$_{Pto}^{ATG}$ may target only a subset of *Arabidopsis* RIN4 that is sufficient to promote *P. syringae* virulence but insufficient to interfere with AvrRpt2-mediated HR. Despite these differences, our data demonstrate that transgenic phenotypes can provide valuable insights into type III effector functions.

Despite the limited structural similarity of HopF2$_{Pto}$ to the ADP ribosyltransferase diphtheria toxin (33), no ADP ribosyltransferase activity could be detected in radiolabeling experiments using purified recombinant RIN4 as a substrate or extracts from HopF2$_{Pto}$-expressing transgenic plants (Fig. S6) (33, 39). These and previously published results suggest that HopF2$_{Pto}$ is not a bona fide ADP ribosyltransferase (33). Nevertheless, amino acid D175 was required for the ability of HopF2$_{Pto}$ to compromise AvrRpt2-induced ETI as well as RIN4 disappearance, indicating that HopF2$_{Pto}$ may catalytically modify RIN4 to promote pathogen virulence. The observation that HopF2$_{Pto}$ can effectively inhibit AvrRpt2-cleavage of RIN4 suggests that the domain of HopF2$_{Pto}$ action may overlap with the AvrRpt2-cleavage sites, RCS1 and/or RCS2. It remains to be determined whether HopF2$_{Pto}$ requires RIN4 to suppress PTI in *Arabidopsis* (Fig. S7) (29, 30). Understanding how HopF2$_{Pto}$ manipulates RIN4 promises to uncover the biochemical function of HopF2$_{Pto}$ as well as functional motifs within the RIN4 protein.

In some bean cultivars, HopF1$_{Pph7}$ is recognized by the R1 resistance protein and therefore acts as an avirulence factor (31, 32). Interestingly, the effector AvrB2$_{Pph7}$ (formerly AvrPphC) from *P. syringae* pv. *phaseolicola* race 7 (1449B) is able to mask the avirulence function of HopF1$_{Pph7}$ in the bean cultivar Canadian Wonder (32). RIN4-like proteins are conserved across the plant kingdom in monocots and dicots. Because AvrB2$_{Pph7}$ is an allele of the AvrB family of TTSEs that can target *Arabidopsis* RIN4, it is intriguing to speculate that both HopF1$_{Pph7}$ and AvrB2$_{Pph7}$ could differentially modify a bean RIN4 ortholog.

The HopF family of proteins has previously been demonstrated to possess HR suppressing activity. HopF1$_{Pph7}$ can suppress the avirulence function of an as yet unidentified *Pph* effector, *avrβ1* in the bean cultivar Tendergreen (31, 32). HopF2$_{Pto}$ has also been demonstrated to suppress the HR-inducing activity of HopA1 (formerly HopPsyA) in *Arabidopsis* WS-0 and *N. tabacum* cv. Xanthi and also BAX-induced PCD in yeast and *N. tabacum* cv. Xanthi as well as the HR induced by *P. fluorescens* expressing AvrRpm1 in *Arabidopsis* (27, 30). Suppression of BAX-induced PCD in yeast and plants would suggest that an additional HopF2$_{Pto}$ target might be broadly conserved across kingdoms. HopF2$_{Pto}$ HR-suppression in transgenic *Arabidopsis* appears to be specific to AvrRpt2, suggesting that the mechanism of action examined in these experiments differs from the aforementioned assays.

Overall, we have identified *Arabidopsis* RIN4 as a major virulence target of the *P. syringae* TTSE HopF2$_{Pto}$. HopF2$_{Pto}$ joins the *P. syringae* TTSEs AvrRpm1, AvrRpt2, and AvrB in targeting *Arabidopsis* RIN4 protein. However, unlike the latter three, HopF2$_{Pto}$ avoids R gene-mediated recognition in the *Arabidopsis* Col-0 accession and can target RIN4 when overexpressed to promote pathogen virulence, demonstrating that RIN4 can serve as a virulence target of TTSE proteins.

Methods

Bacterial Strains, Plasmids, and Plant Material. Bacterial cultures and *Arabidopsis* plants were grown as described in ref. 40. HopF2$_{Pto}$ constructs expressed in *P. syringae* were cloned into the multicopy plasmid pBBR1 MCS-2 (41). *HopF2$_{Pto}$* was cloned with 100 bp upstream of the *SchF* ATG start codon and contains an in-frame hemagglutinin (HA) tag at the C terminus. Point mutations were generated by PCR, and the coding sequence of all constructs was sequenced. The HopZ1a$_{PsyA2}$ *P. syringae*- and HopZ1a$_{PsyA2}^{C216A}$ *E. coli*-expressiwon constructs are described refs. 40–42. HopZ1a$_{PsyA2}^{C216A}$ possesses a mutation in the catalytic cysteine (C216) required for in vitro protease activity and avirulence functions (40, 42). HopF2$_{Pto}$ *E. coli* protein expression constructs were cloned into a modified pET-15b vector (Novagen) (43). RIN4 cloned in pGEX6P-3 (GE Healthcare) was provided by Jeff Dangl.

To make transgenic plants, HopF2$_{Pto}$ and HopF2$_{Pto}^{D175A}$ were cloned into pDB vector (40) with an ATG start codon and in-frame with the C-terminal hemagglutinin (HA) tag. The constructs were sequenced, transformed into *Agrobacterium tumefaciens* GV3-101, and transformed into *Arabidopsis* Col-0 plants by floral dip (44). Dexamethasone treatment was as described in ref. 40. Bacterial enumeration, *in planta* growth assays, HR, and ion leakage were conducted as described in ref. 40.

Protein Expression, Purification, and GST Pull Downs. Recombinant 6xHIS:HopF2$_{Pto}$ and 6xHIS:HopZ1a$_{PsyA2}^{C216A}$ (33, 42) were purified by size-exclusion chromatography using a HiLoad 16/60 Superdex 200 prep grade column (Amersham Biosciences) in PBS buffer (140 mM NaCl, 2.7 mM KCl, 10 mM Na_2HPO_4, 1.8 mM KH_2PO_4) at a flow-rate of 1 mL/min. Recombinant GST:RIN4 was affinity-purified in batch format by glutathione sepharose affinity chromatography using Glutathione Sepharose 4B (GE Healthcare) with two 10-mL washes of both 20 mM Tris (pH 8.0)/50 mM NaCl and 20 mM Tris (pH 8.0)/350 mM NaCl. For GST pull-down assays, 200 μl of binding buffer-equilibrated [20 mM Tris (pH 8.0), 50 mM NaCl] Glutathione Sepharose 4B slurry was incubated with 50 μg of GST:RIN4 or GST alone for 1 h at 4°C. Fifty micrograms of purified recombinant 6xHIS:HopF2$_{Pto}$ was then added and incubated for 1 h at 25°C. Two subsequent 5-min washes were conducted with RIPA buffer [50 mM Tris (pH 7.4), 150 mM NaCl, 1% Nonidet P-40, 0.25% Na deoxycholate] (35). The washed beads were then resuspended in 200 μL of the PBS binding buffer. Twenty microliters of the washed beads was then mixed with SDS/PAGE loading buffer, boiled, resolved on 12% SDS/PAGE gels, and immunoblotted.

In Vitro Cleavage Reactions. Recombinant GST:ROC1, AvrRpt2:HA, and 6xHIS:RIN4 proteins were cloned, expressed, and purified as described in ref. 17. Cleavage reactions were performed in a 50-μL total volume using 1 μg of AvrRpt2:HA, 3 μg of 6xHIS:RIN4, 5 μg of GST:ROC1, and BSA, 6xHIS:HopF2$_{Pto}$, or 6xHIS:HopZ1a$_{PsyA2}^{C216A}$ in PBS buffer (140 mM NaCl, 2.7 mM KCl, Na_2HPO_4, 1.8 mM KH_2PO_4). Reactions were incubated at 25°C for 16 h, terminated with SDS/PAGE loading buffer, resolved on 12% SDS/PAGE gels, and immunoblotted.

Protein Extraction, Immunoprecipitation, and Immunoblotting. *Arabidopsis* leaves were ground in liquid nitrogen and resuspended in the immunoprecipitation (IP) buffer [50 mM Tris·HCl (pH 7.5), 150 mM NaCl, 1% Nonidet P-40, 1% dodecyl maltoside, protease inhibitor mixture (Roche)]. The slurry was incubated on ice for 1 h and centrifuged at 10,000 × *g* for 15 min to clear the debris. Seven hundred fifty micrograms of protein was used in all immunoprecipitation experiments. Protein extracts were incubated in either 50 μL of HA-conjugated magnetic beads (Miltenyi Biotech) or 1 μL of RIN4 polyclonal antibodies, followed by 100 μL of Protein A magnetic beads (Miltenyi Biotech), and incubated for 1 h on ice. Following incubation, magnetic beads were washed with IP buffer according to the manufacturer's instructions. HopF2$_{Pto}$ and RIN4 were detected as described below.

For detection of transgenic HopF2$_{Pto}$:HA, one fully expanded leaf was ground in 500 μL of protein extraction buffer [20 mM Tris·HCl (pH 7.5), 150 mM NaCl, 1 mM EDTA, 1% Triton X-100, 5 mM DTT, plant protease inhibitor (Sigma Aldrich)], briefly vortexed, and then centrifuged at 20,000 × *g* for 10 min at 4 °C. SDS/PAGE loading dye (10×) was added to the supernatants, and samples were resolved on 12% SDS/PAGE gels and blotted onto nitrocellulose. Affinity-purified polyclonal rabbit anti-RIN4 sera (10) was used at a 1:10,000 dilution, anti-HIS (Cell Signaling Technology) was used at 1:4,000, and anti-HA (Roche) was used at 1:15,000.

ACKNOWLEDGMENTS. We thank Dr. David Mackey (Ohio State University) for RIN4 antisera; Dr. Ai-Jiuan Wu and Dr. Jeffrey Dangl (University of North Carolina) for GST:RIN4 protein expression construct, the modified pDB vector, and *rin4*/*rps2*, *rin4*/*rps2*/*rpm1*, *rps2*, and *rpm1 Arabidopsis* seeds; Dr. Brian Staskawicz for *Pto* JL1065 strain; Dr. James Alfano (University of Nebraska, Lincoln) for *Pto* DC3000 *HopF2*$^{-}$ strain; and Dr. Alex Singer for comments on the manuscript. This work was supported by Natural Sciences and Engineering Research Council of Canada and Ontario Graduate Scholarship postgraduate awards (to M.W.), a Natural Sciences and Engineering Research Council of Canada Discovery grant (to D.D.), the Canadian Foundation for Innovation (D.D.), a Canada Research Chair in Plant-Microbe Systems Biology (D.D.), and the Centre for the Analysis of Genome Evolution and Function (D.D.). G.C. and J.E. were supported by U.S. Department of Agriculture–National Research Initiative Grant 2008-00712 (awarded to G.C.). J.E. was also supported by National Science Foundation–Integrative Graduate Education and Research Traineeship Fellowship DGE-0653984.

1. Grant SR, Fisher EJ, Chang JH, Mole BM, Dangl JL (2006) Subterfuge and manipulation: type III effector proteins of phytopathogenic bacteria. *Annu Rev Microbiol* 60:425–429.
2. Jones JDG, Dangl JL (2006) The plant immune system. *Nature* 444:323–329.
3. Nomura K, Melotto M, He SY (2005) Suppression of host defense in compatible plant-*Pseudomonas syringae* interactions. *Curr Opin Plant Biol* 8:361–368.
4. Ma W, Guttman DS (2008) Evolution of prokaryotic and eukaryotic virulence effectors. *Curr Opin Plant Biol* 11:412–419.
5. Chisholm ST, Coaker G, Day B, Staskawicz BJ (2006) Host-microbe interactions: shaping the evolution of the plant immune response. *Cell* 124:803–814.
6. Dangl JL, Jones JDG (2001) Plant pathogens and integrated defence responses to infection. *Nature* 411:826–833.
7. Bent AF, Mackey D (2007) Elicitors, effectors, and R genes: the new paradigm and a lifetime supply of questions. *Annu Rev Phytopathol* 45:399–436.
8. van der Biezen EA, Jones JDG (1998) Plant disease-resistance proteins and the gene-for-gene concept. *Trends Biochem Sci* 23:454–456.
9. Kim MG, et al. (2005) Two *Pseudomonas syringae* type III effectors inhibit RIN4-regulated basal defense in *Arabidopsis*. *Cell* 121:749–759.
10. Mackey D, Holt BF, Wiig A, Dangl JL (2002) RIN4 interacts with *Pseudomonas syringae* type III effector molecules and is required for RPM1-mediated resistance in *Arabidopsis*. *Cell* 108:743–758.
11. Mackey D, Belkhadir Y, Alonso JM, Ecker JR, Dangl JL (2003) *Arabidopsis* RIN4 is a target of the type III virulence effector AvrRpt2 and modulates RPS2-mediated resistance. *Cell* 112:379–389.
12. Axtell MJ, Staskawicz BJ (2003) Initiation of RPS2-specified disease resistance in *Arabidopsis* is coupled to the AvrRpt2-directed elimination of RIN4. *Cell* 112:369–377.
13. Lee CC, et al. (2004) Crystal structure of the type III effector AvrB from *Pseudomonas syringae*. *Structure* 12:487–494.
14. Ong LE, Innes RW (2006) AvrB mutants lose both virulence and avirulence activities on soybean and Arabidopsis. *Mol Microbiol* 60:951–962.
15. Desveaux D, et al. (2007) Type III effector activation via nucleotide binding, phosphorylation, and host target interaction. *PLoS Pathog* 3:456–469.
16. Axtell MJ, Chisholm ST, Dahlbeck D, Staskawicz BJ (2003) Genetic and molecular evidence that the *Pseudomonas syringae* type III effector protein AvrRpt2 is a cysteine protease. *Mol Microbiol* 49:1537–1546.
17. Coaker G, Falick A, Staskawicz B (2005) Activation of a phytopathogenic bacterial effector protein by a eukaryotic cyclophilin. *Science* 308:548–550.
18. Coaker G, Zhu G, Ding Z, Van Doren SR, Staskawicz B (2006) Eukaryotic cyclophilin acts as a molecular switch for effector activation. *Mol Microbiol* 61:1485–1496.
19. Jin P, Wood MD, Wu Y, Xie Z, Katagiri F (2003) Cleavage of the *Pseudomonas syringae* type III effector AvrRpt2 requires a host factor(s) common among eukaryotes and is important for AvrRpt2 localization in the host cell. *Plant Physiol* 133:1072–1082.
20. Chisholm ST, et al. (2005) Molecular characterization of proteolytic cleavage sites of the *Pseudomonas syringae* effector AvrRpt2. *Proc Natl Acad Sci USA* 102:2087–2092.
21. Day B, et al. (2005) Molecular basis for the RIN4 negative regulation of RPS2 disease resistance. *Plant Cell* 17:292–1305.
22. Kim HS, et al. (2005) The *Pseudomonas syringae* effector AvrRpt2 cleaves its C-terminally acylated target, RIN4, from *Arabidopsis* membranes to block RPM1 activation. *Proc Natl Acad Sci USA* 102:6496–6501.
23. Belkhadir Y, Nimchuk Z, Hubert DA, Mackey D, Dangl JL (2004) *Arabidopsis* RIN4 negatively regulates disease resistance mediated by RPS2 and RPM1 downstream or independent of the NDR1 signal modulator and is not required for the virulence functions of bacterial type III effectors AvrRpt2 or AvrRpm1. *Plant Cell* 16:2822–2835.
24. van der Hoorn RA, Kamoun S (2008) From guard to decoy: a new model for perception of plant pathogen effectors. *Plant Cell* 20:2009–2017.
25. Shan L, et al. (2004) The *hopPtoF* locus of *Pseudomonas syringae* pv. *tomato* DC3000 encodes a type III chaperone and a cognate effector. *Mol Plant Microbe Interact* 17: 447–455.
26. Robert-Seilaniantz A, Shan L, Zhou J-M, Tang X (2006) The *Pseudomonas syringae* pv. *tomato* DC3000 type III effector HopF2 has a putative myristoylation site required for its avirulence and virulence functions. *Mol Plant Microbe Interact* 19:130–138.
27. Jamir Y, et al. (2004) Identification of *Pseudomonas syringae* type III effectors that can suppress programmed cell death in plants and yeast. *Plant J* 37:554–565.
28. Oh HS, Collmer A (2005) Basal resistance against bacteria in *Nicotiana benthamiana* leaves is accompanied by reduced vascular staining and suppressed by multiple *Pseudomonas syringae* type III secretion system effector proteins. *Plant J* 44:348–359.
29. Li X, et al. (2005) Flagellin induces innate immunity in nonhost interactions that is suppressed by *Pseudomonas syringae* effectors. *Proc Natl Acad Sci USA* 102: 12990–12995.
30. Gou M, Tiang F, Wamboldt Y, Alfano JR (2009) The majority of the type III effector inventory of *Pseudomonas syringae* pv. *tomato* DC3000 can suppress plant immunity. *Mol Plant Microbe Interact* 22:1069–1080.
31. Jackson RW, et al. (1999) Identification of a pathogenicity island, which contains genes for virulence and avirulence, on a large native plasmid in the bean pathogen *Pseudomonas syringae* pathovar *phaseolicola*. *Proc Natl Acad Sci USA* 96: 10875–10880.
32. Tsiamis G, et al. (2000) Cultivar-specific avirulence and virulence functions assigned to *avrPphF* in *Pseudomonas syringae* pv. *phaseolicola*, the cause of bean halo-blight disease. *EMBO J* 19:3204–3214.
33. Singer AU, et al. (2004) Crystal structures of the type III effector protein AvrPphF and its chaperone reveal residues required for plant pathogenesis. *Structure* 12: 1669–1681.
34. Aoyama T, Chua N-H (1997) A glucocorticoid-mediated transcriptional induction system in transgenic plants. *Plant J* 11:605–612.
35. Elion EA, Wang Y (2004) Making protein immunoprecipitates. *Methods Mol Biol* 284: 1–14.
36. Ritter C, Dangl JL (1996) Interference between two specific pathogen recognition events mediated by distinct plant disease resistance genes. *Plant Cell* 8:251–257.
37. Lim MT, Kunkel BN (2005) The *Pseudomonas syringae avrRpt2* gene contributes to virulence on tomato. *Mol Plant Microbe Interact* 18:626–633.
38. Kubori T, Galan JE (2003) Temporal regulation of *Salmonella* virulence effector function by proteasome-dependent protein degradation. *Cell* 115:333–342.
39. Coburn J, Wyatt RT, Iglewski BH, Gill DM (1989) Several GTP-binding proteins, including p21c-H-ras, are preferred substrates of *Pseudomonas aeruginosa* exoenzyme S. *J Biol Chem* 264:9004–9008.
40. Lewis JD, Abada W, Ma W, Guttman DS, Desveaux D (2008) The HopZ family of *Pseudomonas syringae* type III effectors require myristoylation for virulence and avirulence functions in Arabidopsis thaliana. *J Bacteriol* 190:2880–2891.
41. Kovach ME, et al. (1995) Four new derivatives of the broad-host-range cloning vector pBBR1MCS, carrying different antibiotic-resistance cassettes. *Gene* 166:175–176.
42. Ma W, Dong FF, Stavrinides J, Guttman DS (2006) Type III effector diversification via both pathoadaptation and horizontal transfer in response to a coevolutionary arms race. *PLoS Genet* 2:2131–2142.
43. Zuo Y, et al. (2007) Crystal structure of RNase T, an exoribonuclease involved in tRNA maturation and end turnover. *Structure* 15:417–428.
44. Clough SJ, Bent AF (1998) Floral dip: a simplified method for Agrobacterium-mediated transformation of *Arabidopsis thaliana*. *Plant J* 16:735–743.